RESEARCH ARTICLE

Key Points:

- Time series data from automated chemical sensors reveal the complexity of glacial fjord biogeochemistry and the influence of meltwater
- *In situ* nitrate and DSi sensors deployed for the first time in an Arctic fjord reveal complexity that would be missed with manual samples
- In-fjord processing results in decoupling between nitrate and DSi and nonconservative behavior

High-Resolution Sensors Reveal Nitrate and Dissolved Silica Dynamics in an Arctic Fjord

Alexander D. Beaton[1], Katharine R. Hendry[2,3], Jade E. Hatton[2,4], Matthew D. Patey[1], Matthew Mowlem[1], Geraldine Clinton-Bailey[1], Patricia Lopez-Garcia[1], E. Malcolm S. Woodward[5], and Lorenz Meire[6,7]

[1]National Oceanography Centre, Southampton, England, [2]School of Earth Sciences, University of Bristol, Bristol, UK, [3]British Antarctic Survey, Cambridge, UK, [4]Department of Ecology, Charles University, Prague, Czechia, [5]Plymouth Marine Laboratory, Plymouth, UK, [6]Greenland Climate Research Centre (GCRC), Greenland Institute of Natural Resources, Nuuk, Greenland, [7]Department of Estuarine and Delta Systems, Royal Netherlands Institute for Sea Research, Yerseke, The Netherlands

Abstract Subglacial weathering releases biologically important nutrients into meltwaters that have the potential to influence downstream ecosystems. There is a need to understand how accelerated glacial retreat could impact biogeochemical cycling in coastal regions in the near future. However, fjords—important gateways connecting the Greenland ice sheet and coastal oceans—are highly heterogeneous environments both in space and time. Here, we investigate temporal variability of nutrient dynamics in a glacier-fed fjord (Nuup Kangerlua, Greenland) using a high resolution record of nitrate + nitrite ($\sum NO_x$) and dissolved silica (DSi), coupled with temperature and salinity, using submersible in situ sensors. During a 3-month monitoring period (14th June to 13 September 2019), $\sum NO_x$ varied between 0.05 and 10.07 μM (±0.2 μM), whereas DSi varied between 0.35 and 14.98 μM (±0.5 μM). Both nutrients started low (following the spring bloom) and increased throughout the monitoring period. Several large peaks in both nutrients were observed, and these can largely be associated with meltwater runoff and upwelling events. Peaks in DSi were likely the direct result of glacial meltwater pulses, whereas elevated $\sum NO_x$ concentrations in the fjord system were likely the result of meltwater-induced upwelling of marine sources. However, we did not observe a case of simple conservative mixing, suggesting that other processes in the fjord system (e.g., differential biological uptake and remineralization) may decouple the relationship between the two nutrients. This data set was used to investigate the biogeochemical impact of changes in glacier meltwater input throughout the melt season.

Plain Language Summary Ice sheets and glaciers are melting at an increasing rate resulting in changes to the volume and composition of glacial meltwater entering Arctic coastal waters. Here, ecosystems play a role in absorbing atmospheric carbon dioxide and help support important fisheries. Dissolved nutrients from glacial meltwater have an important effect on these ecosystems by helping to support biological productivity. Some nutrients enter the fjord directly from melting glaciers, whereas others are brought to the surface from deep in the fjord by rising meltwater entering below the surface (where glaciers directly meet the fjord). Both sources are thought to be impacted by changes in meltwater volumes. However, collecting water samples in Greenlandic fjord environments is logistically challenging, making it difficult to predict how ecosystems will respond to changes in glacier meltwater input. To help address this, we deployed some recently developed cutting-edge sensors designed to automatically conduct high-quality measurements of nutrients for several months. The sensors operated like miniature laboratories; they could calibrate themselves and automatically filter, process, and analyze water samples. This resulted in a twice-daily record of nutrient concentrations over a 3-month period, allowing us unprecedented insight to the complexity of nutrient concentrations in a glacial fjord.

1. Introduction

A combination of physical and chemical weathering in Arctic subglacial environments releases both dissolved and reactive solid phases of biologically important elements, which are then advected downstream via glacial meltwater (Hopwood et al., 2020; Wadham et al., 2019). Such nutrients can be directly biologically available in dissolved form, or become so through dissolution and further processing, and include dissolved silica or silicic acid (DSi) (Hatton, Hendry, Hawkings, Wadham, Kohler, et al., 2019; Hatton, Hendry, Hawkings, Wadham,

E. Hatton, Matthew D. Patey, Matthew Mowlem, Lorenz Meire
Investigation: Alexander D. Beaton, Katharine R. Hendry, Lorenz Meire
Methodology: Alexander D. Beaton, Katharine R. Hendry, Jade E. Hatton, Matthew D. Patey, Matthew Mowlem, Geraldine Clinton-Bailey, Patricia Lopez-Garcia, E. Malcolm S. Woodward, Lorenz Meire
Project administration: Alexander D. Beaton, Katharine R. Hendry, Matthew Mowlem, Lorenz Meire
Resources: Alexander D. Beaton, Katharine R. Hendry, Matthew Mowlem, Lorenz Meire
Software: Alexander D. Beaton
Validation: Alexander D. Beaton, Katharine R. Hendry, Jade E. Hatton, Matthew D. Patey, Lorenz Meire
Visualization: Alexander D. Beaton, Katharine R. Hendry, Lorenz Meire
Writing – original draft: Alexander D. Beaton, Katharine R. Hendry, Lorenz Meire
Writing – review & editing: Alexander D. Beaton, Katharine R. Hendry, Jade E. Hatton, Matthew D. Patey, Matthew Mowlem, Patricia Lopez-Garcia, E. Malcolm S. Woodward, Lorenz Meire

Opfergelt, et al., 2019; Hawkings et al., 2017, 2018; Meire et al., 2016), phosphorus (Hawkings et al., 2016), and trace elements such as iron (Aciego et al., 2015; Bhatia et al., 2013; Hawkings et al., 2014; Krisch et al., 2021). There is clear motivation, given the recent acceleration in glacial melting rates, to understand and quantify how changing meltwater rates may affect nutrient release and productivity in downstream ecosystems and any climate feedback that might be at play. The recent acceleration in melting of the Greenland ice sheet (e.g., (Karlsson et al., 2021; Shepherd et al., 2020) is likely driving an increase in the supply of meltwater and entrained nutrients to downstream ecosystems, which could impact downstream ecosystems and carbon cycling and result in further climatically important feedback processes. However, the link between meltwater flux, nutrient delivery to fjordic and coastal waters, and the promotion of marine biological production will likely depend on nonconservative processes within fjords, including abiotic cycling (e.g., sorption and dissolution) and biological uptake (Hopwood et al., 2015) in addition to fjord geometry, hydrology, mixing, and circulation (Bendtsen et al., 2015; Hopwood et al., 2018; Oliver et al., 2020).

Both nitrate and DSi are important nutrients for fjord primary production in southwest Greenland, including Nuup Kangerlua (e.g., Meire et al., 2016). Nitrate is often the main limiting nutrient within fjords, but its main source is not derived directly from glacial meltwater. Nitrate concentrations in glacial meltwater are relatively low (0–5 μM (Wadham et al., 2016),) and nitrate supplied directly from glacial meltwater is not considered an important nutrient source for coastal ecosystems (e.g., Cape et al., 2019; Meire et al., 2016). However, buoyant subsurface meltwater plumes from marine terminating glaciers are able to entrain nitrate from deep water (Cape et al., 2019; Kanna et al., 2018; Meire et al., 2017). Glacial meltwater from marine terminating glaciers therefore influences the supply of nitrate to fjord surface waters and is thought to sustain summer blooms in Nuup Kangerlua (Meire et al., 2016, 2017, 2023).

In contrast, subglacially derived meltwater is rich in DSi (concentrations ranging up to 40 μM in subglacial discharge waters compared to coastal surface and deep seawater concentrations that range from <2 μM to 9–10 μM, respectively (Hendry et al., 2019; Hopwood et al., 2020)) as a result of subglacial weathering. Glacial meltwater concentrations of DSi are generally higher than those found in Arctic coastal seawater, meaning that glacial meltwater represents a direct source of additional DSi to the Arctic marine environment (Meire et al., 2016). This comes both via runoff from land terminating glaciers and subsurface meltwater plumes from marine terminating glaciers. Diatoms, an important group of algae growing in Greenlandic fjords (Krawczyk et al., 2018) and coastal waters, form siliceous cell walls and so have a fundamental requirement for DSi, which can be seasonally limiting in Greenlandic fjords including Nuup Kangerlua (Krause et al., 2019).

Nutrient cycling processes within fjords are poorly understood largely because of the limited observations by spot sampling that can result in an incomplete picture of the complex hydrological and biological dynamics involved. All currently available nutrient data are derived from bottle samples collected from research vessels, and such low temporal resolution is likely to miss high-frequency events (e.g., meltwater pulses, internal wave-driven, or upwelling events) that may offer key insights into fjord processes. Continuous monitoring of water chemistry in fjord environments is logistically challenging and is difficult to achieve at high-resolution without robust and analytically stable *in situ* sensors (Bagshaw et al., 2016). Recent advances in microfluidic or lab-on-chip (LOC) technology have led to the development of a range of *in situ* nutrient analyzers that offer high-quality, stable, long-term (several months) deployments suitable for the high turbidity conditions found within fjords. In contrast to UV nitrate sensors, LOC sensors are able to filter small volumes of sample water prior to analysis, allowing them to measure highly turbid glacial meltwaters. In addition, the sensors use sensitive wet chemical analyses, which make them suitable for glacial fjord waters where concentrations are in the low micromolar to submicromolar range. They carry onboard calibration standards and blank solutions, allowing them to self-calibrate and maintain accuracy over deployments of several months to years (Beaton et al., 2012; Beaton, Mowlem, et al., 2017). Here, we present new data sets with high temporal resolution obtained from a deployment of *in situ* nitrate + nitrite (referred to from here as $\sum NO_x$) and DSi sensors for 91 days in a glacial-fed Arctic fjord. The study has two aims: first, to demonstrate the use of autonomous sensors in challenging subarctic coastal environments and second to gain insights into the complexity of biogeochemistry of the fjord environment. Our findings reveal short-term trends associated with meltwater pulses, upwelling events, and other in-fjord processes that could not be captured with traditional manual water sampling methods.
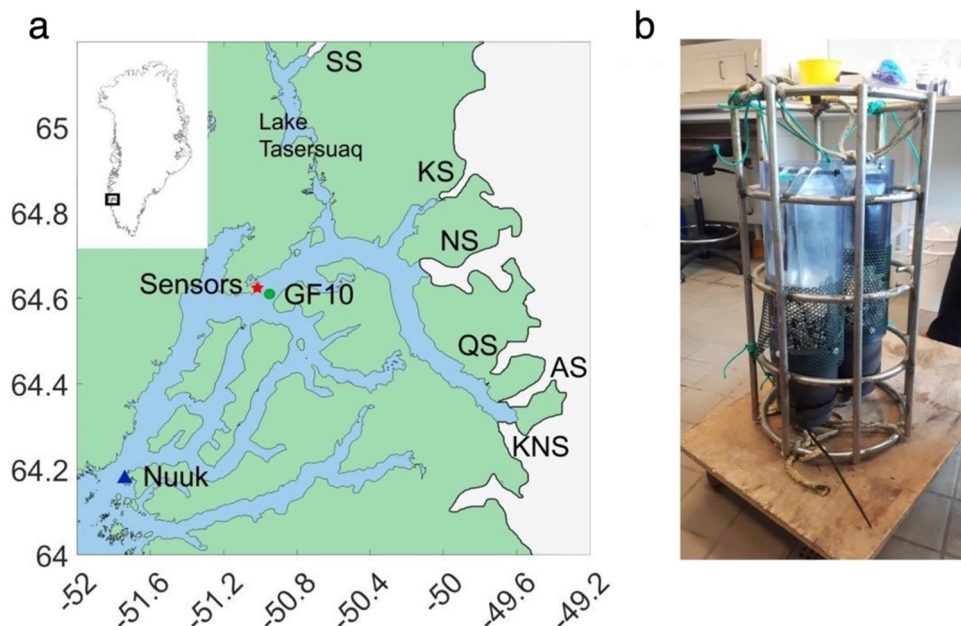
Figure 1. (a) Map of deployment site showing the fjord system with each of the glaciers draining into the fjord, the sensor deployment location (red star), the nearest CTD station GF10 (green dot), and Nuuk (blue triangle); (b) photograph of the stainless steel sensor frame containing both LOC sensors. The battery was mounted directly below the frame.

2. Materials and Methods

2.1. Field Site

Nuup Kangerlua (Godthåbsfjord) is located close to Nuuk on the southwest coast of Greenland (Figure 1a). It is 190 km long and connects via the continental shelf to the Labrador Sea. It is fed by three marine terminating tidewater glaciers (Narsap Sermia (NS), Akullersuup Sermia (AS), and Kangiata Nunaata Sermia (KNS), inputting freshwater at depth into the fjord) and three land terminating glaciers (Saqqap Sermersua (SS), Kangilinnguata Sermia (KS), and Qamanaarsuup Sermia (QS) inputting freshwater at the surface of the fjord via lakes and rivers).

The sensors were deployed at a site approximately 47 km downstream from the terminus of NS and 28 km downstream from the point at which meltwater from glacier SS drains into the main fjord via Lake Tasersuaq. The site is expected to receive a strong influence from glacial meltwater (Mortensen et al., 2020).

2.2. Lab-On-Chip Sensors

The lab-on-chip (LOC) $\sum NO_x$ and DSi sensors used in this study (developed at the National Oceanography Centre, Southampton, UK) perform wet chemical colorimetric analysis on polymer microfluidic chips (Beaton et al., 2011, 2012, 2022). These sensors are well suited to deployment in the glacial fjord environment for several reasons detailed below. The sensors use well-characterized and sensitive colorimetric assays (the Griess assay for $\sum NO_x$ analysis and the molybdenum blue assay for DSi (Grasshoff et al., 2009). Microfluidics minimizes reagent consumption such that all waste from the chemical analysis is stored onboard the sensor and reduces fluidic pumping volume to minimize power consumption and sample volume. Optical measurements are performed using low-power components (light-emitting diodes and photodiodes). The sensors feature a pressure-compensated housing that allows them to be deployed to depths of up to 6000 m. Both sensors carried a blank solution and onboard calibration standards (10 μM for $\sum NO_x$, 10 and 20 μM for DSi) that were analyzed along with every measurement, allowing them to maintain accuracy over several months of deployment. The blank and standards were made from artificial seawater at a salinity of 17.5. The nitrate sensor measured total nitrate plus nitrite ($\sum NO_x$), although nitrite is expected to be close to or below limit of detection in this environment (e.g., Hatton, Ng, Beaton, et al., 2023). The $\sum NO_x$ sensor was previously demonstrated in rivers, estuaries, the deep

sea, and a proglacial steam (Beaton et al., 2012, 2017a, 2017b, 2022). The DSi sensor, which is almost identical in design, has previously been deployed in riverine and ocean (Beaton et al., 2025) environments.

2.3. Sensor Deployment

The LOC $\sum NO_x$ and DSi sensors were mounted to a stainless steel deployment frame (Figure 1b) designed to protect the instrumentation from passing icebergs and direct contact with rocky cliff edge of the fjord. Both sensors were powered by a single 12 V 60 Ah pressure compensated submersible lead acid battery (DeepSea Power & Light), which was mounted below the frame. The sensor frame was suspended from a stainless steel wire anchored directly to the bedrock cliff at the side of the fjord (64.610°N, 51.038°W, bottom depth 20 m, dropping rapidly to 580 m into the fjord) and secured to an average depth of 5 m (however varying due to tide between 2 and 8 m). The sensors were deployed on 14th June 2019 and recovered on 13th September 2019.

The sensors were programmed to draw in ambient water (through 0.45 μm pore-size 13 mm diameter MILLEX polyethersulfone inlet filters fitted to each sensor) and measure its nutrient concentration every 12 hr. Each measurement was accompanied by the measurement of an onboard calibration standard and a blank solution (artificial seawater). Data were stored onboard each sensor (on a micro secure digital (SD) memory card) for download upon recovery.

A Sea-Bird SBE 37 MicroCAT was mounted inside a cage next to the nutrient sensors, and measured conductivity, temperature and depth (CTD) with a 10-min resolution. In addition, a CTD water column profile was taken at site GF10, approximately 2 km away from the sensor deployment site (64.610°N, 50.958°W, ~580 m water depth) at the end of the monitoring period (13 September 2019). All CTD sensors were calibrated by the manufacturer prior to deployment. The $\sum NO_x$ sensor, DSi sensor, and CTD operated as intended for the full monitoring period with the nutrient sensors performing two measurements per 24-hr period for 91 days.

2.4. Manually Collected Samples

Spot samples were taken in surface waters (~3 m) at a site 2 km from the deployment site (sampling site GF10; Figure 1) from an underway pumping system on 13 September 2019. Acid-cleaned reinforced PVC tubing was connected to a Towfish system mounted from the side of the vessel (MV Tulu), and a Teflon bellows pump (AstiPure II, Saint Gobain) was used pump fluid to a sampling point on deck. Additional samples were collected using a Niskin bottle from different depths on the same day and on two additional dates in June and July. The samples were filtered through 0.2 μm Supor filters and frozen for transport back to the UK. Samples for inorganic nutrients were analyzed at the Plymouth Marine Laboratory. The samples were defrosted by heating in a warm water bath for 45 min from frozen and then equilibrating to room temperature for another 30 min before analysis (Becker et al., 2020). $\sum NO_x$ and DSi analyses were carried out using a SEAL analytical AAIII segmented flow colorimetric autoanalyzer (Woodward & Rees, 2001). Seawater nutrient reference materials (KANSO Ltd. Japan) were also analyzed to assess analyzer performance and for final data quality control. The typical uncertainty of the analytical results was 2%–3%.

3. Results

3.1. Nutrient Samples and Sensor Comparison

Niskin bottle samples for nutrient analysis collected at the same location on 13th September 2019 (Table 1) show $\sum NO_x$ is depleted at 3 m but increasing with depth, whereas DSi is highest at the 3 m sample. Additional samples taken on 13th July show nitrate depleted at the surface (1 m) and increasing with depth (5 m), whereas DSi is enriched in the surface sample but lower at 5 m depth.

$\sum NO_x$ and DSi concentrations from these samples have been plotted (Figure 2) in order to compare to the concentrations reported by the sensors. Note that a direct comparison with the concentrations measured by the nutrient sensors is complicated by the fact that the depth of the mooring varied with the tide (see Supporting Information S1), and the sampling location is not exactly colocated with the mooring.

Table 1
Nutrient Analysis Data From Water Samples Collected at Station GF10 Using Either Niskin Bottles or Underway Towfish

Date (2019)	Depth (m)	DSi (µM)	$\sum NO_x$ (µM)
14th June	1	7.96	0.48
13th July	1	6.38	0.47
13th July	5	2.39	1.14
13th September	3	10.09	0.10
13th September	20	1.51	5.86
13th September	200	4.61	9.92

3.2. Temperature and Salinity Variability Through Time

Temperature started low (1°C) but showed a general increase accompanied by several peaks (up to 7°C) during the monitoring period (Figure 2c). Salinity started at 31 and gradually decreased throughout the summer to a minimum of 15 in early August before recovering again to 29 at the end of the monitoring period (Figure 2d). Short-term fluctuations in salinity and temperature are likely a result of tidal fluctuations and changes in the depth of the sensor frame (between 2 and 8 m)

3.3. Nutrient Variability Through Time

For ease of interpretation, the time series data have been split into six periods (A-F) chosen due to the presence of noteworthy changes in either $\sum NO_x$ or DSi concentrations.

3.3.1. $\sum NO_x$

Apart from two short peaks, $\sum NO_x$ remained close to zero until mid-July (Figure 2e: Period A) during which time the water was relatively cold and saline. $\sum NO_x$ began to rise in late July (Period B) as salinity dropped peaking up to approximately 9 µM. $\sum NO_x$ then dropped back to almost zero during a large DSi spike in mid-August (Period C), which was accompanied by a drop in temperature and salinity. $\sum NO_x$ increased again after this, with peaks over 9 µM (Period D), and fluctuated before dropping again in late August to approximately 3 µM (Period E). This drop was also accompanied by a decrease in salinity, a spike in DSi (see Section 3.2.2), and this time a spike in temperature. $\sum NO_x$ peaked again in early September (Period F) with relatively little change in temperature or salinity or DSi. During the monitoring period, there were five distinct peaks during which $\sum NO_x$ concentrations measured by the sensor (at 5 m water depth) reached (but never exceeded) the concentrations found in deeper fjord waters (Table 1).

3.3.2. Dissolved Silica

Dissolved silica (DSi) concentrations recorded at 5 m water depth in Nuup Kangerlua (Figure 2f) frequently exceeded those found in deeper waters (Table 1). DSi concentrations started low varying between 0.35 and 1.71 µM for the first 14 days (start of Period A). DSi then entered a period of fluctuation between 1.0 and 5.7 µM (middle of Period A). DSi concentrations then rose from 17th July onward as salinity dropped (end of Period A and Period B) culminating in a large spike in DSi concentration (15 µM) on 8th August (Period C). This DSi spike was associated with a drop in $\sum NO_x$, which decreased from 4 µM on 6th August to 0.4 µM on 8th August. Soon afterward, DSi concentrations dropped dramatically reaching 1.5 µM by 11th August. Both $\sum NO_x$ and DSi remained low until 12th August, when both began to increase. There was a short spike in DSi (14.4 µM) on 23rd August (Period E) that was also associated with a spike in temperature, decrease in salinity, and low $\sum NO_x$ concentrations. DSi remained relatively constant during the subsequent large spike in $\sum NO_x$ (Period F).

3.4. Water Column Profile and Nutrient Samples

The CTD water column profile from 13th September 2019 (Figure 3) shows a shallow fresh layer in the top 20 m, overlying saltier water (salinity 33.4), with a subsurface temperature maximum of 3°C at approximately 60 m that decreases to approximately 1°C at depth (Figures 3a and 3b). Turbidity largely reflects salinity with a strong surface peak in the top 10 m, and there is a chlorophyll *a* maximum between 10 and 30 m water depth (Figures 3c and 3d).

4. Discussion

4.1. Seasonal Upwelling and Meltwater Pulse Events Recorded in Nutrients

Previous studies have shown that elevated $\sum NO_x$ concentrations in the upper water column of fjords fed by marine terminating glaciers to be largely a result of upwelled marine waters (e.g., Cape et al., 2019; Meire et al., 2017), whereas elevated DSi concentrations originate mostly from surface meltwater runoff (Hopwood
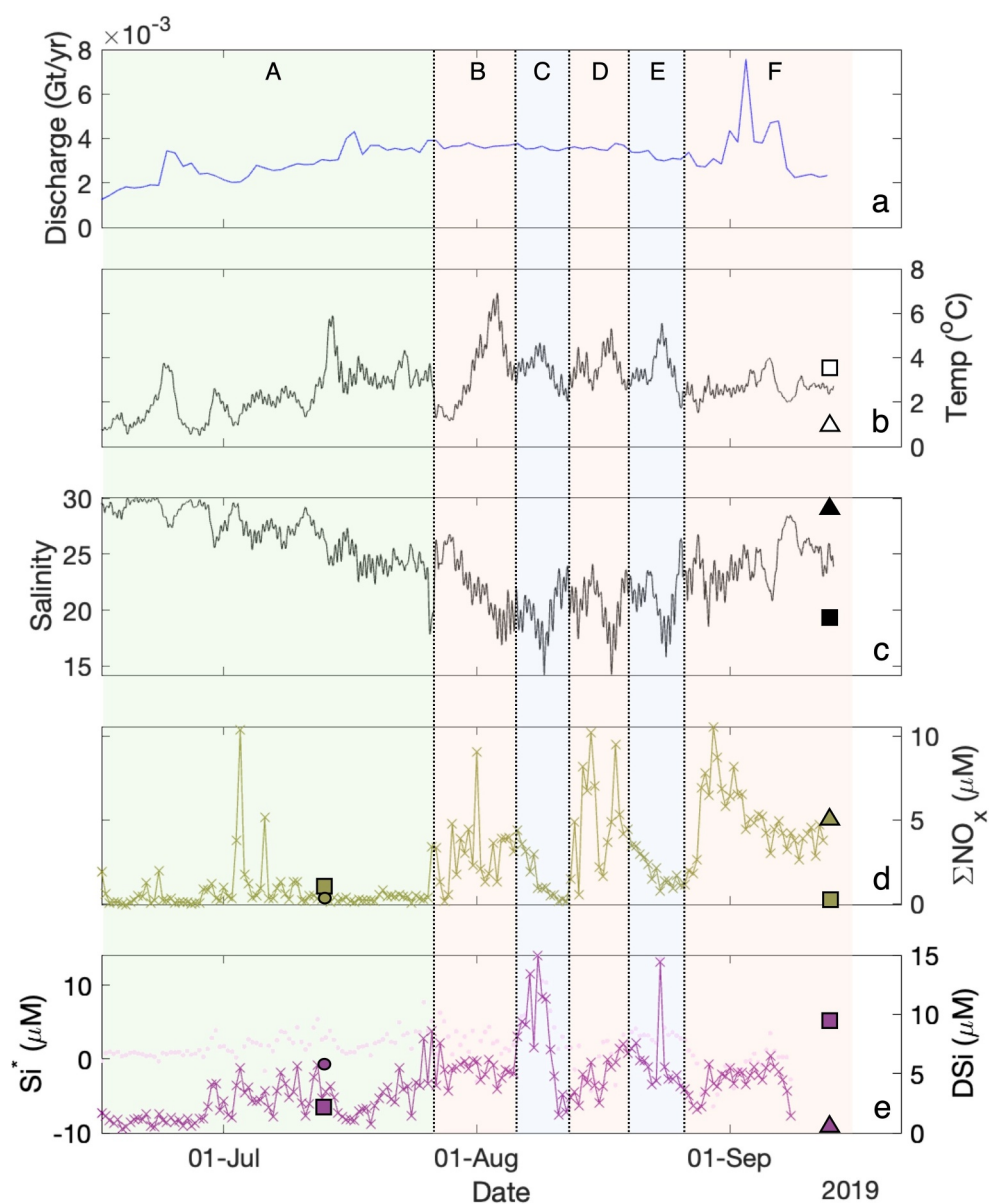
Figure 2. Time series environmental data and data from sensors at 2–8 m water depth at study site in Nuup Kangerlua. (a): Total meltwater discharge from KNS, AS, NS, QS, and KS (RACMO, data from Mankoff et al., 2020). (b): Water temperature. (c): Water salinity. (d): $\sum NO_x$. (e): DSi (purple crosses) and Si* (pink dots), where Si* = [DSi] - [$\sum NO_x$]. Solid symbols show water properties at nearby GF10 station (triangles 20 m water depth, squares 3–5 m water depth, circles 1 m water depth) on 13 September 2019 (when the sensors were recovered). Nutrient samples from an additional sampling date on 13th July are also plotted. The time series has been partitioned into six periods (a)–(f) to aid interpretation.

et al., 2020; Meire et al., 2016). Nuup Kangerlua is characterized by a low average baseline discharge rate punctuated by rapid increases over short periods of time (Van As et al., 2014).

Using our high-resolution time series of $\sum NO_x$, DSi, temperature and salinity (in conjunction with knowledge of end-member concentrations of deep marine water and freshwater glacial runoff (e.g., Hopwood et al., 2016; Meire et al., 2016), we can infer the presence of upwelling and surface meltwater runoff events that occurred during the monitoring period as well as additional events or processes that do not fit into this simple model. Upwelling at or close to the sensor location can be triggered by specific ice-dammed lake drainage events (Kjeldsen et al., 2014) leading to increased subsurface discharge from marine terminating glaciers or by increased subglacial discharge caused by increased melting. However, wind-driven and tidal mixing could locally impact upwelling of
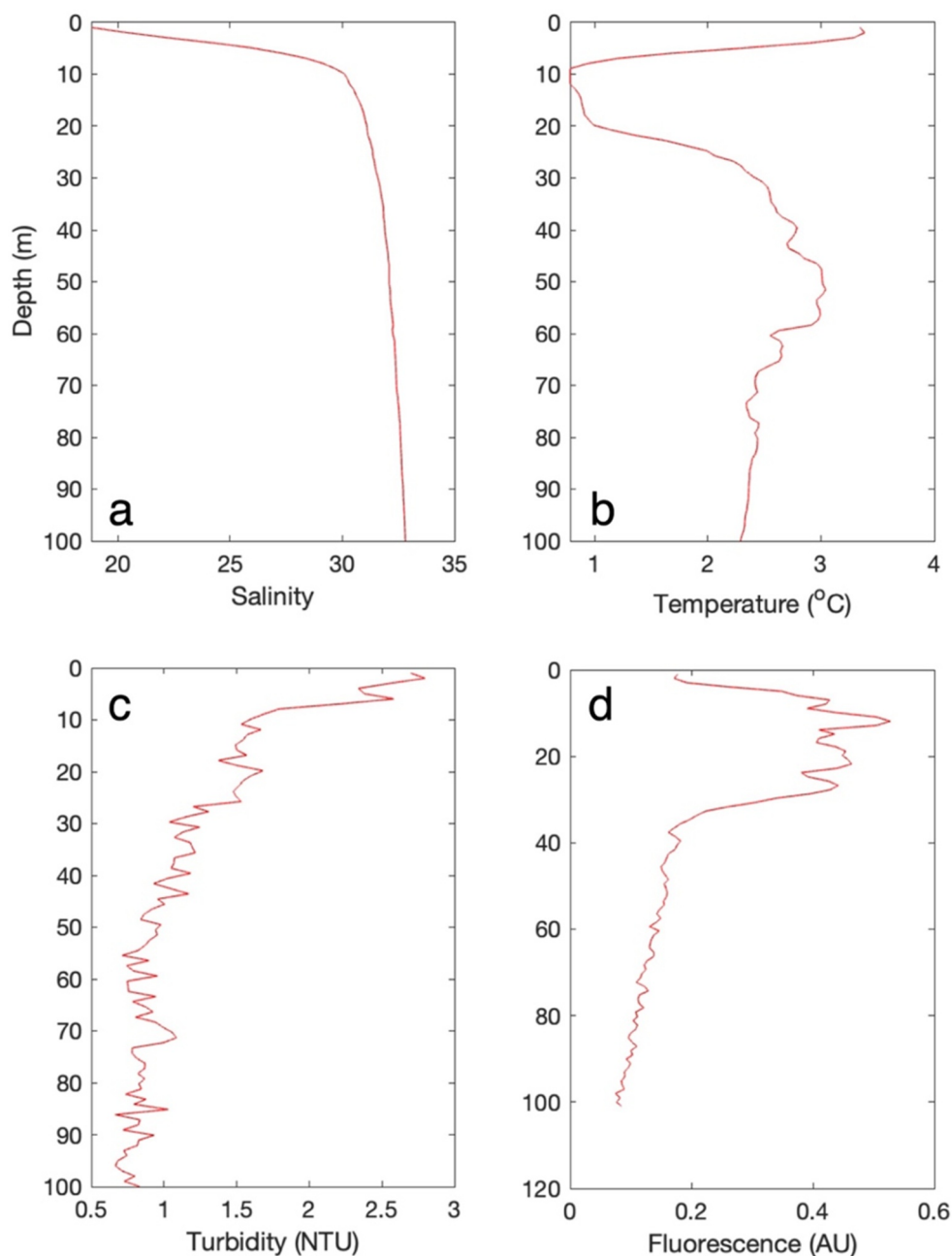
Figure 3. Profiles collected from Station GF10 in September 2019, showing (a) Salinity; (b) Temperature; (c) Turbidity; and (d) Fluorescence for top 100 m.

subsurface waters as well (Mortensen et al., 2011). In contrast, surface meltwater runoff events are the result of increased discharge from land terminating glaciers and the lakes that they drain into (e.g., Lake Tasersuaq) as well as iceberg melt after periods of intense calving.

We characterize upwelling or mixing events as the presence of water with elevated $\sum NO_x$ and salinity. Five distinct spikes in $\sum NO_x$ (in Periods A, B, D, and F) came close to the 9 µM measured in our sample collected at 200 m (Table 1). Of these, events A and D are associated with drops in temperature and spikes in salinity and could be interpreted as being influenced by upwelling or mixing events. During Period F, $\sum NO_x$ spiked while salinity was elevated, but DSi and temperature remained relatively flat. There are peaks in the maximum wind speed (Supporting Information S1) at the beginning of Periods B and D, which could indicate stronger wind-
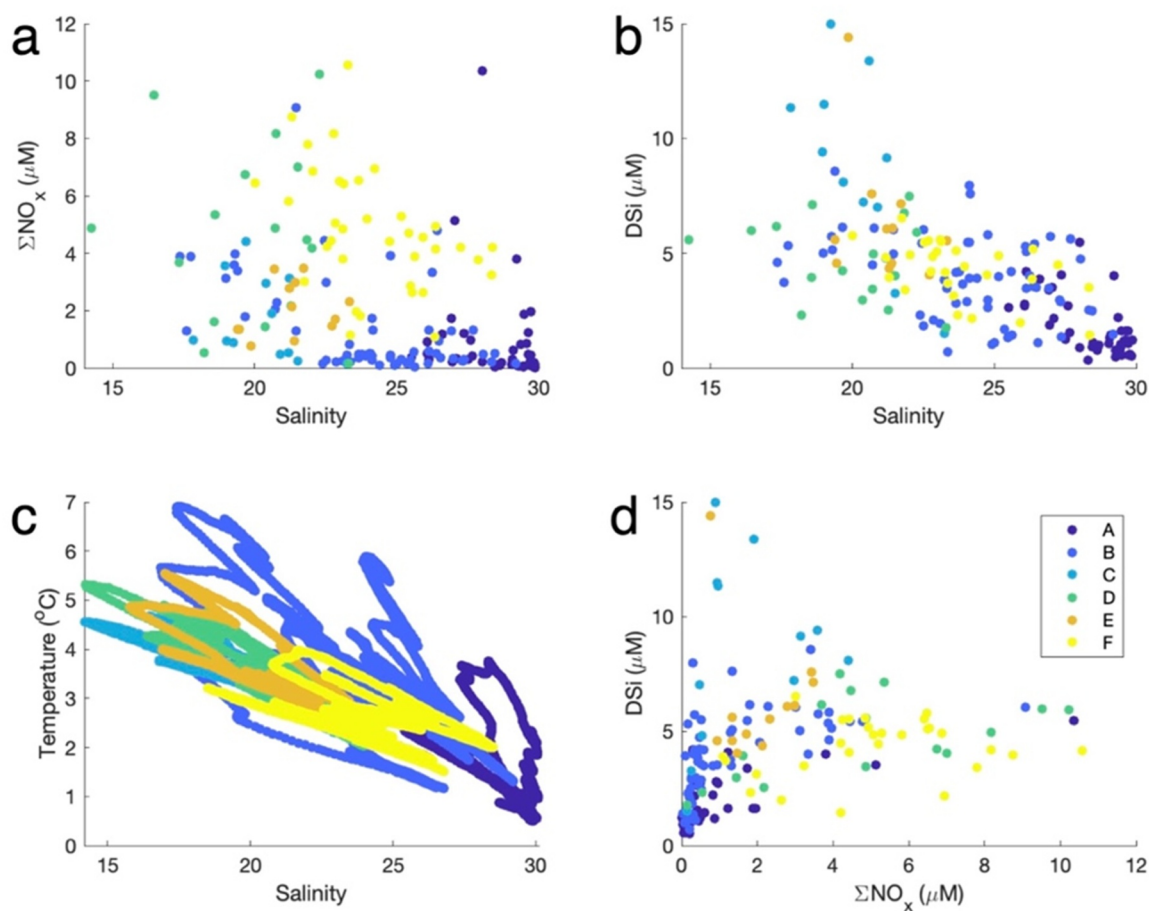
Figure 4. Scatter plots for each of the periods A-F identified in the time series (Figure 2) with the linear fit R^2 values indicated for the full data set. (a) $\sum$NOx versus salinity $R^2 = 0.15$; (b) DSi versus salinity $R^2 = 0.42$; (c) Temperature versus Salinity $R^2 = 0.63$; (d): DSi versus $\sum$NOx $R^2 = 0.12$.

driven mixing at these times. Period F is also associated with prolonged peaks in high maximum wind speeds in addition to enhanced ice discharge from the marine-terminating glaciers into Nuup Kanglerlua (Figures 2a and 2b).

In contrast, DSi concentrations that are distinctly above those of the deep water (i.e., 8 μM at 400 m; Hopwood et al., 2016) coupled with low $\sum$NO$_x$, low salinity, and higher water temperatures indicate the dominance of surface meltwater runoff over meltwater-induced upwelling. This situation clearly occurred during Period C (a large DSi spike associated with low salinity and low $\sum$NO$_x$) and Period E (a shorter salinity spike associated with low $\sum$NO$_x$, low salinity and a spike in water temperature). DSi concentrations in local freshwater runoff (e.g., 31 μM in Lake Tasersuaq; Hopwood et al., 2016) are higher than those in marine derived waters, and satellite images (Supporting Information S1) confirm the influx of sediments from Lake Tasersuaq during this part of mid-August (Period C). This supports the idea of enhanced surface water runoff during part of the meltwater season.

Although we are able to identify the signature of clear upwelling and surface meltwater runoff events, signals that do not necessarily fit this simple model (e.g. Period F)—as well as temporal changes in the relationships between each of the parameters (Figure 4) point toward the presence of additional processes decoupling the relationship between $\sum$NO$_x$, DSi, salinity, and temperature in the fjord system, which will be discussed below.

4.2. Coupling and Decoupling of T, S, $\sum$NO$_x$, and DSi

The relationship between temperature, salinity, $\sum$NO$_x$, and DSi evolved throughout the melt season (Figure 4), indicating shifts in the sources and sinks of the two nutrients in relation to upwelling and stratification caused by meltwater runoff.

Si* (defined as Si* = [DSi] - [$\sum NO_x$]) is more commonly used in open ocean settings to trace diatom production (Sarmiento et al., 2004) but here it is used to track the relationship between $\sum NO_x$ and DSi in the fjord environment. Si* diverged from DSi over the monitoring period (Figure 2f). Despite initially displaying a positive relationship (Figure 4), a decoupling occurred between $\sum NO_x$ and DSi that grew stronger throughout the monitoring period (Figures 2e and 2f), indicating the presence of different processes influencing the cycling of the two nutrients and an evolution of these processes throughout the melt season. We propose three processes that could be responsible for this.

4.2.1. Change of Source Waters (Marine vs. Glacial) and Their Relative Composition

Although $\sum NO_x$ largely comes from upwelled marine sources, the relationship between $\sum NO_x$ and salinity is weaker (Figure 4a) than the relationship between DSi and salinity (Figure 4b) possibly due to the relative influence of different upwelling sources and changes in depth of subsurface plume related to variations in overall melt volume. Although our data suggest that DSi is derived from low salinity meltwater (Figure 4b), there is also some scatter in the relationship with very high DSi values (c. 15 μM) in mid-salinity range (18–24).

The T-S plot (Figure 4c) shows that more saline waters are always colder, but the strength of this relationship diminishes throughout the monitoring period (i.e., temperature starts to vary less with salinity such that the temperature does not increase to the same extent during reductions in salinity). Surface warming in coastal waters in the fjord and within the proglacial systems could introduce some variability in the water temperature that would not be reflected in the salinity or nutrient data.

Temperature and salinity decoupling has been observed previously in other studies. Kjeldsen et al. (2014) showed how the drainage of ice-dammed glacial lakes influences conductivity and temperature of fjord surface waters using data from a CTD deployed close to our monitoring site (in 2009). Following outburst floods caused by lake drainage events, they observed a decrease in temperature over several days, followed by a rapid increase in salinity that stayed high for several days while temperature gradually increased again.

It is also possible that there is a shift in the composition of the marine source. Marine saline surface water could also be advected in-fjord during some periods (Mortensen et al., 2020), which could also introduce some variability in nutrient content of the high-salinity endmember.

4.2.2. Differential Biological Uptake and Remineralization

Both $\sum NO_x$ and DSi concentrations were low at the start of the monitoring period likely because of nutrient depletion during the spring bloom. The two nutrients initially showed a positive relationship (when nutrient levels were still relatively low) but this relationship broke down later in the monitoring period as nutrient levels increased (Figure 4d). Although $\sum NO_x$ is required by all phytoplankton, only some organisms (i.e., diatoms in this case) take up DSi. Differential biological uptake (and subsequent differential remineralization) means that we would not necessarily expect a linear relationship between $\sum NO_x$ and DSi.

4.2.3. Dissolution of Abiotic Particulates

Another potential source of DSi into the fjord system is the dissolution of biogenic silica (BSi) largely from diatoms and amorphous particulate silica (ASi) in the water column and at the fjord water-sediment interface. ASi has been shown to dominate silica export from the Greenland ice sheet with concentrations of ASi in glacial meltwater reported to be several times higher than those of DSi (Hawkings et al., 2018).

ASi is up to two orders of magnitude more soluble in saline waters compared to freshwater (Icenhower & Dove, 2000). It has been shown to dissolve on timescales of days to weeks (Kato & Kitano, 1968) in seawater at 20°C. We would expect this dissolution rate to be much slower at fjord water temperatures (Hawkings et al., 2017a, Hawkings et al., 2014), given the dissolution rate coefficient for amorphous diatom frustules in seawater approximately doubles with a 10°C in temperature (Kamatani, 1982). However, incubation experiments using frozen glacial sediments reveal that dissolution rates show a weak dependence on temperature between 4 and 11°C (Zhu et al., 2024) and are similar to those in experiments carried out at room temperature (Hawkings et al., 2017a, Hawkings et al., 2014). Dissolution of glacially derived ASi as it reaches the salinity gradient may result in elevated levels of DSi in the fjord system (Hatton, Ng, Beaton, et al., 2023; Hatton, Ng, Meire, et al., 2023) and therefore contribute to the gradual change in Si* (Figure 2f). Given the transit distances from the

marine termini to the study location (~45–80 km), this additional source of DSi to the fjord system (and its variation over time) may be responsible for the observed nonconservative behavior (Figure 4). Similarly, dissolution of detrital biogenic silica from previous diatom blooms could also contribute to elevated DSi in the fjord system.

5. Conclusions

Our observations have shown $\sum NO_x$ and DSi concentrations in a glacier-fed Greenlandic fjord to be highly variable, offering a glimpse into the complexity of glacial fjord biogeochemistry and the influence of meltwater. Reliance on monthly or weekly spot samples will clearly miss many of the short-term changes in nutrient concentrations. The physical and chemical signature of large spikes in $\sum NO_x$ and DSi suggests that they are associated with meltwater, be it direct surface runoff (in the case of DSi) or via entrainment of marine-sourced nutrients by subsurface subglacial discharge (in the case of $\sum NO_x$).

However, complexities relating to other processes likely add to the decoupling of the two nutrients, including abiotic and biological uptake and dissolution processes. This kind of complexity can only be captured using high resolution sensors. Although there is a clear requirement for high frequency measurements in fjords in order to capture this complexity, multiple monitoring locations in a fjord system such as Nuup Kangerlua would aid our understanding on special variability. This will be the focus of future studies. Further insight could be gained from measurements of isotopes (e.g., Hatton, Ng, Meire, et al., 2023) as well as the development of models to understand underlying mechanisms behind the variations. Collection and analysis of these data sets will have consequences for our understanding of how changes in glacial meltwater runoff affects nutrient availability in polar fjords.

Lab-on-chip technology for automated *in situ* nutrient measurements has now been shown to be robust enough for multiple-month-long deployment in remote polar environments. More widespread application of this technology will increase our understanding by providing automated high-resolution data in hard-to-reach locations.

Conflict of Interest

The authors declare the following competing financial interest(s): ADB and MM are cofounders and employees of Clearwater Sensors. The remaining authors declare that the research was conducted in the absence of any commercial or financial relationships that could be construed as a potential conflict of interest.

Data Availability Statement

The data sets generated and analyzed during this study are available through the Pangaea® data repository at https://doi.org/10.1594/PANGAEA.974184 (Beaton et al., 2025a), https://doi.org/10.1594/PANGAEA.974183 (Beaton et al., 2025b), https://doi.org/10.1594/PANGAEA.974182 (Beaton et al., 2025c), and https://doi.org/10.1594/PANGAEA.974171 (Beaton et al., 2025d).

References

Aciego, S. M., Stevenson, E. I., & Arendt, C. A. (2015). Climate versus geological controls on glacial meltwater micronutrient production in southern Greenland. *Earth and Planetary*, *424*, 51–58. https://doi.org/10.1016/j.epsl.2015.05.017

Bagshaw, E. A., Beaton, A., Wadham, J. L., Mowlem, M., Hawkings, J. R., & Tranter, M. (2016). Chemical sensors for in situ data collection in the cryosphere. *TrAC, Trends in Analytical Chemistry*, *82*, 348–357. https://doi.org/10.1016/j.trac.2016.06.016

Beaton, A. D., Birchill, A. J., Clinton-Bailey, G. S., Plueddemann, A. J., White, S., Pabortsava, K., & Martin, A. P. (2025). Lab-on-chip nitrate + nitrite and silicate sensors on Ocean Observing Initiative (OOI) Southern Ocean Surface Mooring from December 2018 to January 2020 (Version 1) [Dataset]. *NERC EDS British Oceanographic Data Centre NOC*. https://doi.org/10.5285/2E94021D-6D35-3419-E063-7086ABC03AC0

Beaton, A. D., Cardwell, C. L., Thomas, R. S., Sieben, V. J., Legiret, F. E., Waugh, E. M., et al. (2012). Lab-on-chip measurement of nitrate and nitrite for in situ analysis of natural waters. *Environmental Science and Technology*, *46*(17), 9548–9556. https://doi.org/10.1021/es300419u

Beaton, A. D., Hendry, K. R., Hatton, J. E., & Meire, L. (2025a). CTD profile measurements from a glacier-fed fjord conducted close to a sensor deployment site during cruise TU19 (Nuup Kangerlua, Greenland) [dataset]. *PANGAEA*. https://doi.org/10.1594/PANGAEA.974184

Beaton, A. D., Hendry, K. R., Hatton, J. E., & Meire, L. (2025b). Temperature and salinity measurements from a moored CTD deployed in a glacier-fed fjord (Nuup Kangerlua, Greenland) between June and September 2019 [dataset]. *PANGAEA*. https://doi.org/10.1594/PANGAEA.974183

Beaton, A. D., Hendry, K. R., Hatton, J. E., & Meire, L. (2025c). Time series measurements from a lab-on-chip dissolved silica (DSi) sensor deployed in a glacier-fed fjord (Nuup Kangerlua, Greenland) between June and September 2019 [dataset]. *PANGAEA*. https://doi.org/10.1594/PANGAEA.974182

Beaton, A. D., Hendry, K. R., Hatton, J. E., & Meire, L. (2025d). Time series measurements from a lab-on-chip nitrate sensor deployed in a glacier-fed fjord (Nuup Kangerlua, Greenland) between June and September 2019 [dataset]. *PANGAEA*. https://doi.org/10.1594/PANGAEA.974171

Beaton, A. D., Mowlem, M. C., Purdie, D. A., Panton, A., & Owsianka, D. R. (2017). *Nitrate and nitrite data from a National Oceanography Centre (NOC) lab-on-chip (LOC) analyser at Knapp Mill (Hampshire Avon) British Oceanographic data Centre - Natural environment research Council*. British Oceanographic Data Centre - Natural Environment Research Council. https://doi.org/10.5285/47f09d73-b5aa-0c3b-e0536c86abc02aa2

Beaton, A. D., Schaap, A. M., Pascal, R., Hanz, R., Martincic, U., Cardwell, C. L., et al. (2022). Lab-on-Chip for in situ analysis of nutrients in the deep sea. *ACS Sensors*, *7*(1), 89–98. https://doi.org/10.1021/acssensors.1c01685

Beaton, A. D., Sieben, V. J., Floquet, C. F. A., Waugh, E. M., Bey, S. A. K., Ogilvie, I. R. G., et al. (2011). An automated microfluidic colourimetric sensor applied in situ to determine nitrite concentration. *Sensors and Actuators B: Chemical*, *156*(2), 1009–1014. https://doi.org/10.1016/j.snb.2011.02.042

Beaton, A. D., Wadham, J. L., Hawkings, J., Bagshaw, E. A., Lamarche-Gagnon, G., Mowlem, M. C., & Tranter, M. (2017b). High-resolution in situ measurement of nitrate in runoff from the Greenland ice sheet. *Environmental Science and Technology*, *51*(21), 12518–12527. https://doi.org/10.1021/acs.est.7b03121

Becker, S., Aoyama, M., Woodward, E. M. S., Bakker, K., Coverly, S., Mahaffey, C., & Tanhua, T. (2020). GO-SHIP repeat hydrography nutrient manual: The precise and accurate determination of dissolved inorganic nutrients in seawater, using continuous flow analysis methods. *Frontiers in Marine Science*, *7*(October). https://doi.org/10.3389/fmars.2020.581790

Bendtsen, J., Mortensen, J., & Rysgaard, S. (2015). Modelling subglacial discharge and its influence on ocean heat transport in Arctic fjords. *Ocean Dynamics*, *65*(11), 1535–1546. https://doi.org/10.1007/s10236-015-0883-1

Bhatia, M. P., Kujawinski, E. B., Das, S. B., Breier, C. F., Henderson, P. B., & Charette, M. A. (2013). Greenland meltwater as a significant and potentially bioavailable source of iron to the ocean. *Nature Geoscience*, *6*(4), 274–278. https://doi.org/10.1038/ngeo1746

Cape, M. R., Straneo, F., Beaird, N., Bundy, R. M., & Charette, M. A. (2019). Nutrient release to oceans from buoyancy-driven upwelling at Greenland tidewater glaciers. *Nature Geoscience*, *12*(1), 34–39. https://doi.org/10.1038/s41561-018-0268-4

Grasshoff, K., Kremling, K., & Ehrhardt, M. (2009). *Methods of seawater analysis*. Wiley.

Hatton, J. E., Hendry, K. R., Hawkings, J. R., Wadham, J. L., Kohler, T. J., Stibal, M., et al. (2019). Investigation of subglacial weathering under the Greenland Ice Sheet using silicon isotopes. *Geochimica et Cosmochimica Acta*, *247*, 191–206.

Hatton, J. E., Hendry, K. R., Hawkings, J. R., Wadham, J. L., Opfergelt, S., Kohler, T. J., et al. (2019). Silicon isotopes in Arctic and sub-Arctic glacial meltwaters: The role of subglacial weathering in the silicon cycle. *Proceedings of the Royal Society A: Mathematical, Physical and Engineering Sciences*, *475*(2228), 20190098. https://doi.org/10.1098/RSPA.2019.0098

Hatton, J. E., Ng, H. C., Beaton, A., Hawkings, J., Leng, M. J., Meire, L., et al. (2023). Hydrographic and biogeochemical data from Godhäbsfjord and Ameralik fjord, SW Greenland, 2018-2019 [dataset]. PANGAEA. https://doi.org/10.1594/PANGAEA.930217

Hatton, J. E., Ng, H. C., Meire, L., Woodward, E. M. S., Leng, M. J., Coath, C. D., et al. (2023). Silicon isotopes highlight the role of glaciated fjords in modifying coastal waters. *Journal of Geophysical Research: Biogeosciences*, *128*(7). https://doi.org/10.1029/2022JG007242

Hawkings, J., Hatton, J. E., Hendry, K. R., De Souza, G. F., Wadham, J. L., Ivanovic, R., et al. (2018). The silicon cycle impacted by past ice sheets. *Nature Communications*, *9*(1), 1–10. https://doi.org/10.1038/s41467-018-05689-1

Hawkings, J., Wadham, J., Tranter, M., Telling, J., Bagshaw, E., Beaton, A., et al. (2016). The Greenland Ice Sheet as a hot spot of phosphorus weathering and export in the Arctic. *Global Biogeochemical Cycles*, *30*(2), 191–210. https://doi.org/10.1002/2015gb005237

Hawkings, J., Wadham, J. L., Benning, L. G., Hendry, K. R., Tranter, M., Tedstone, A., et al. (2017a). Ice sheets as a missing source of silica to the polar oceans. *Nature Communications*, *8*(1), 14198. https://doi.org/10.1038/ncomms14198

Hawkings, J., Wadham, J. L., Benning, L. G., Hendry, K. R., Tranter, M., Tedstone, A., et al. (2017b). Ice sheets as a missing source of silica to the polar oceans. *Nature Communications*, *8*(1), 14198. https://doi.org/10.1038/ncomms14198

Hawkings, J., Wadham, J. L., Tranter, M., Raiswell, R., Benning, L. G., Statham, P. J., et al. (2014). Ice sheets as a significant source of highly reactive nanoparticulate iron to the oceans. *Nature Communications*, *5*(May), 3929. https://doi.org/10.1038/ncomms4929

Hendry, K. R., Huvenne, V. A. I., Robinson, L. F., Annett, A., Badger, M., Jacobel, A. W., et al. (2019). The biogeochemical impact of glacial meltwater from Southwest Greenland. *Progress in Oceanography*, *176*(October 2018), 102126. https://doi.org/10.1016/j.pocean.2019.102126

Hopwood, M., Bacon, S., Arendt, K., Connelly, D. P., & Statham, P. J. (2015). Glacial meltwater from Greenland is not likely to be an important source of Fe to the North Atlantic. *Biogeochemistry*, *124*(1–3), 1–11. https://doi.org/10.1007/s10533-015-0091-6

Hopwood, M., Carroll, D., Browning, T. J., Meire, L., Mortensen, J., Krisch, S., & Achterberg, E. P. (2018). Non-linear response of summertime marine productivity to increased meltwater discharge around Greenland. *Nature Communications*, *9*(1), 3256. https://doi.org/10.1038/s41467-018-05488-8

Hopwood, M., Carroll, D., Dunse, T., Hodson, A., Holding, J. M., Iriarte, J. L., et al. (2020). Review article: How does glacier discharge affect marine biogeochemistry and primary production in the Arctic? *The Cryosphere*, *14*(4), 1347–1383. https://doi.org/10.5194/tc-14-1347-2020

Hopwood, M. J., Connelly, D. P., Arendt, K. E., Juul-Pedersen, T., Stinchcombe, M. C., Meire, L., et al. (2016). Seasonal changes in Fe along a glaciated Greenlandic fjord. *Front. Earth Sci.*, *4*, 15. https://doi.org/10.3389/feart.2016.00015

Icenhower, J. P., & Dove, P. M. (2000). The dissolution kinetics of amorphous silica into sodium chloride solutions: Effects of temperature and ionic strength. *Geochimica et Cosmochimica Acta*, *64*(24), 4193–4203. https://doi.org/10.1016/s0016-7037(00)00487-7

Kamatani, A. (1982). Dissolution rates of silica from diatoms decomposing at various temperatures. *Marine Biology*, *68*(1), 91–96. https://doi.org/10.1007/bf00393146

Kanna, N., Sugiyama, S., Ohashi, Y., Sakakibara, D., Fukamachi, Y., & Nomura, D. (2018). Upwelling of macronutrients and dissolved inorganic carbon by a subglacial freshwater driven plume in Bowdoin fjord, Northwestern Greenland. *Journal of Geophysical Research: Biogeosciences*, *123*(5), 1666–1682. https://doi.org/10.1029/2017JG004248

Karlsson, N. B., Solgaard, A. M., Mankoff, K. D., Gillet-Chaulet, F., MacGregor, J. A., Box, J. E., et al. (2021). A first constraint on basal melt-water production of the Greenland ice sheet. *Nature Communications*, *12*(1), 1–10. https://doi.org/10.1038/s41467-021-23739-z

Kato, K., & Kitano, Y. (1968). Solubility and dissolution rate of amorphous silica in distilled and sea water at 20°C. *Journal of the Oceanographical Society of Japan*, *24*(4), 147–152. https://doi.org/10.5928/kaiyou1942.24.147

Kjeldsen, K. K., Mortensen, J., Bendtsen, J., Petersen, D., Lennert, K., & Rysgaard, S. (2014). Ice-dammed lake drainage cools and raises surface salinities in a tidewater outlet glacier fjord, west Greenland. *Journal of Geophysics Research Earth Surface*, *119*(6), 1310–1321. https://doi.org/10.1002/2013JF003034

Krause, J. W., Schulz, I. K., Rowe, K. A., Dobbins, W., Winding, M. H. S., Sejr, M. K., et al. (2019). Silicic acid limitation drives bloom termination and potential carbon sequestration in an Arctic bloom. *Scientific Reports*, *9*(1), 1–11. https://doi.org/10.1038/s41598-019-44587-4

Krisch, S., Hopwood, M. J., Schaffer, J., Al-Hashem, A., Höfer, J., Rutgers van der Loeff, M., et al. (2021). The 79°N Glacier cavity modulates subglacial iron export to the NE Greenland Shelf. *Nature Communications*, *12*(1), 3030. https://doi.org/10.1038/s41467-021-23093-0

Mankoff, K. D., Solgaard, A., Colgan, W., Ahlstrøm, A. P., Khan, S. A., & Fausto, R. S. (2020). Greenland Ice Sheet solid ice discharge from 1986 through March 2020. *Earth System Science Data*, *12*(2), 1367–1383. https://doi.org/10.5194/essd-12-1367-2020

Meire, L., Meire, P., Struyf, E., Krawczyk, D. W., Arendt, K. E., Yde, J. C., et al. (2016). High export of dissolved silica from the Greenland Ice Sheet. *Geophysical Research Letters*, *43*(17), 9173–9182. https://doi.org/10.1002/2016GL070191

Meire, L., Mortensen, J., Meire, P., Juul-Pedersen, T., Sejr, M. K., Rysgaard, S., et al. (2017). Marine-terminating glaciers sustain high productivity in Greenland fjords. *Global Change Biology*, *23*(12), 5344–5357. https://doi.org/10.1111/gcb.13801

Meire, L., Paulsen, M. L., Meire, P., Rysgaard, S., Hopwood, M. J., Sejr, M. K., et al. (2023). Glacier retreat alters downstream fjord ecosystem structure and function in Greenland. *Nature Geoscience*, *16*(8), 671–674. https://doi.org/10.1038/s41561-023-01218-y

Mortensen, J., Lennert, K., Bendtsen, J., & Rysgaard, S. (2011). Heat sources for glacial melt in a sub-Arctic fjord (Godthåbsfjord) in contact with the Greenland Ice Sheet. *Journal of Geophysical Research*, *116*(C1). https://doi.org/10.1029/2010jc006528

Mortensen, J., Rysgaard, S., Bendtsen, J., Lennert, K., Kanzow, T., Lund, H., & Meire, L. (2020). Subglacial discharge and its down-fjord transformation in west Greenland fjords with an ice Mélange. *Journal of Geophysical Research: Oceans*, *125*(9), 1–13. https://doi.org/10.1029/2020JC016301

Oliver, H., Castelao, R. M., Wang, C., & Yager, P. L. (2020). Meltwater-enhanced nutrient export from Greenland's glacial fjords: A sensitivity analysis. *Journal of Geophysical Research: Oceans*, *125*(7), 1–18. https://doi.org/10.1029/2020JC016185

Sarmiento, J. L., Gruber, N., Brzezinski, M. A., & Dunne, J. P. (2004). High-latitude controls of thermocline nutrients and low latitude biological productivity. *Nature*, *427*(6969), 56–60. https://doi.org/10.1038/nature02127

Shepherd, A., Ivins, E., Rignot, E., Smith, B., Van Den Broeke, M., Velicogna, I., et al. (2020). Mass balance of the Greenland ice sheet from 1992 to 2018. *Nature*, *579*(7798), 233–239. https://doi.org/10.1038/s41586-019-1855-2

Van As, D., Andersen, M. L., Petersen, D., Fettweis, X., Van Angelen, J. H., Lenaerts, J. T. M., et al. (2014). Increasing meltwater discharge from the Nuuk region of the Greenland ice sheet and implications for mass balance (1960–2012). *Journal of Glaciology*, *60*(220), 314–322. https://doi.org/10.3189/2014jog13j065

Wadham, J. L., Hawkings, J., Telling, J., Chandler, D., Alcock, J., O'Donnell, E., et al. (2016). Sources, cycling and export of nitrogen on the Greenland Ice Sheet. *Biogeosciences*, *13*(22), 6339–6352. https://doi.org/10.5194/bg-13-6339-2016

Wadham, J. L., Hawkings, J. R., Tarasov, L., Gregoire, L. J., Spencer, R. G. M., Gutjahr, M., et al. (2019). Ice sheets matter for the global carbon cycle. *Nature Communications*, *10*(1). https://doi.org/10.1038/s41467-019-11394-4

Woodward, E. M. S., & Rees, A. P. (2001). Nutrient distributions in an anticyclonic eddy in the northeast Atlantic ocean, with reference to nanomolar ammonium concentrations. *Deep-Sea Research Part II Topical Studies in Oceanography*, *48*(4–5), 775–793. https://doi.org/10.1016/S0967-0645(00)00097-7

Zhu, X., Hopwood, M. J., Laufer-Meiser, K., & Achterberg, E. P. (2024). Incubation experiments characterize turbid glacier plumes as a major source of Mn and Co, and a minor source of Fe and Si, to seawater. *Global Biogeochemical Cycles*, *38*(10), e2024GB008144. https://doi.org/10.1029/2024gb008144

References From the Supporting Information

Greenland Ecosystem Monitoring. (2024). ClimateBasis Nuuk - wind - wind speed @ 200 cm - 10 min maximum (m/s) (Version 1.0). [Dataset] [CC-BY-SA-4.0]. Greenland Ecosystem Monitoring. https://doi.org/10.17897/QB0M-FD72